

Review

Opportunities in main group molecular electronics

Matthew O. Hight¹ and Timothy A. Su  ^{1,2,*}

Main group molecular electronics is an emerging area that investigates quantum transport through main group backbones within molecular junctions. It merges two rapidly advancing fields: main group chemical synthesis and single-molecule electronics. Though the current scope of quantum transport studies in main group molecules is much narrower than it is for organic molecules, they have led to major advances in single-molecule electronics, including the discovery of stereoelectronic switching, destructive σ -quantum interference, and intramolecular London dispersion interactions in single-molecule junctions. This review article provides an overview of this subfield and charts a path to the future of main group molecular electronics.

The case for main group molecular electronics

The field of molecular electronics was created out of an interest to use molecules as the active elements (i.e., resistors, rectifiers, wires, switches) in electronic circuitry [1–8]. Though realizing practical molecular electronics has remained a key goal, the interests of the field have expanded toward discovering novel **quantum transport** (see **Glossary**) phenomena that emerge only at the molecular scale [9–11]. To date, most **molecular junction** studies have involved organic molecules (Figure 1A,B, Key figure). While **main group elements** are commonly used to bind wires to electrodes [12], create covalent electrode–molecule contacts [13–17], and augment the transport characteristics of π -conjugated organic wires [18–21], it is almost always in service of studying π -conjugated organic backbones (Figure 1A).

In our view, main group element backbones deserve considerably more attention in molecular electronic studies (Figure 1C). Like organic wires, their covalent bond composition should make them physically robust to the repeated breaking and forming of single-molecule junctions over metal electrodes, which is a challenge for organometallic wires, whose ligands may dissociate and bind to metal electrodes [22]. They can have high energy bonding orbitals whose interactions may lead to novel quantum transport phenomena. Indeed, the small subset of quantum transport studies on σ -bonded main group backbones have contributed major advances in the field, far beyond the generalizations made from organic wires. The study of straight-chain silicon and germanium wires showed for the first time that σ -bonds can be as conductive as π -conjugated phenylene rings on a length-dependent basis in quantum transport contexts [23–25]. The strong conjugation along the tetrel σ -bond axis enabled the first demonstration of stereoelectronic switching, where conductance can be toggled between high and low conducting states by mechanically controlling σ -bond stereoelectronics [24,25]. Meanwhile, it is now appreciated that we can make main group σ -bonds far more resistive than the canonical alkane insulator by introducing strong polarity into the backbone [26], harnessing intramolecular London dispersion interactions to control backbone geometry [27], and imposing internal backbone constraints [28]. *Cisoid*-constrained Si backbones led to the discovery of **destructive quantum interference (DQI)** in σ -bonded systems, a quantum transport phenomena assumed to be the domain of π -conjugated organic wires. Studying

Highlights

Led by advances in fundamental inorganic synthesis, the scope of known main group compounds has grown in crescendo. These compounds exhibit attractive physical properties for molecular electronics due to the distinctive structure and bonding aspects of main group elements.

Meanwhile, the study of conductive molecular junctions is growing in sophistication, where more quantum transport features can be probed than ever before. These techniques are becoming increasingly accessible.

New paradigms in molecular electronics have been created from studying main group compounds in molecular junctions, including the discovery of σ -destructive quantum interference, stereoelectronic switching, and intramolecular London dispersion interactions in single-molecule junctions.

Now is the moment to dive deeply into the emerging area of main group molecular electronics.

¹Department of Chemistry, University of California, Riverside, CA 92521, USA

²Materials Science & Engineering Program, University of California, Riverside, CA 92521, USA

*Correspondence:
timothys@ucr.edu (T.A. Su).



Key figure

The state of the art and future directions for main group compounds in single-molecule junctions

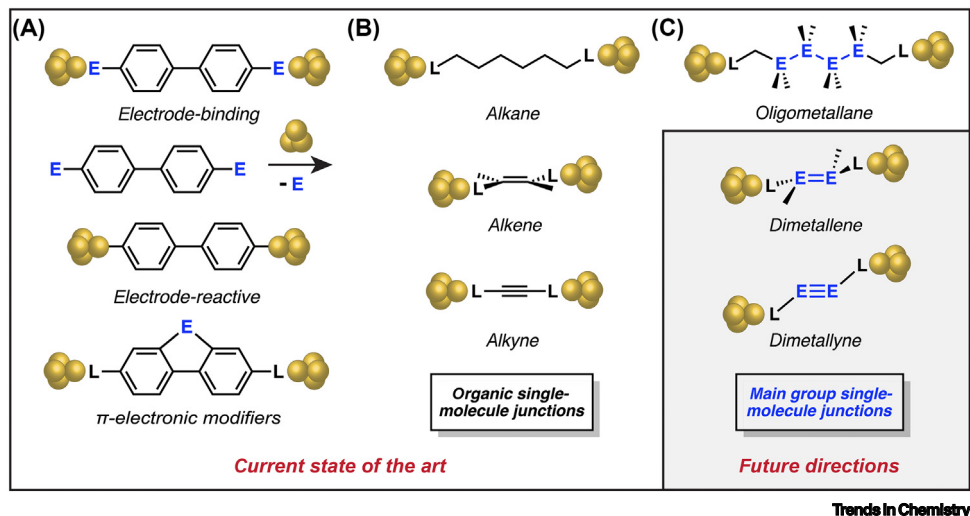


Figure 1. (A) Main group elements (E) are most commonly used in auxiliary roles for organic molecule electronics. In electrode-binding roles, pnictogens and chalcogens can form covalent and dative linkages between the organic backbone and electrode. In electrode-reactive roles, *p*-block substituents such as E = $-\text{SnMe}_3$, $-\text{SiMe}_3$, $-\text{N}_2$, $-\text{I}$, $-\text{B}(\text{OH})_2$ are replaced by Au atoms in transmetallation or oxidative addition-type reactions to give organic wires with direct C–Au covalent linkages. As π -electronic modifiers, the main group element can raise or lower frontier molecular orbital energies to tune charge transport behavior. L signifies an electrode-linking group. (B) Organic wires of increasing bond order from alkanes, alkenes, to alkynes. Organic wires have been the focus of single-molecule electronics. (C) This review article explores the current state of the art and future work of studying molecular backbones composed of main group elements, including heavy analogs of alkanes (**oligometallanes**), alkenes (dimetallenes), and alkynes (dimetallynes).

single-molecule conductance in main group backbones has thus uncovered novel quantum transport phenomena that would have been difficult, if not impossible, to discover in organic backbones.

This belief motivates the present article, where we discuss the current state and future directions for an emerging area of work that we have termed ‘main group molecular electronics’. This article takes a forward-looking perspective that focuses on new quantum transport phenomena that may emerge from exploring untapped areas of fundamental main group chemistry in single-molecule junctions studied in the context of **scanning tunneling microscopy break-junction (STM-BJ)** experiments. Comprehensive summaries on existing work in this area [29,30] and the basics of single-molecule conductance measurements and quantum transport in molecular junctions [6,7,9,11,31] have been published elsewhere. We will first describe how seemingly well-explored properties of saturated main group compounds have given rise to wholly new phenomena in quantum transport contexts, in some cases, overturning the assumptions of a carbon-centric field. This article will detail the exciting questions regarding saturated main group backbones that have opened from these studies, then chart a path to exploring unsaturated main group compounds in single-molecule electronics (Figure 1C).

Saturated main group backbones

While many main group compounds have been synthesized over the past several decades, only a small fraction of them have been measured in single-molecule junctions. Saturated chains and

Glossary**Destructive quantum interference (DQI):**

phase cancellation between transmitting molecular orbitals that annuls charge carrier amplitude. While DQI occurs between many orbitals in essentially all molecules, it significantly impacts molecular junction conductance if it influences the electronic transmission probability near the Fermi energy of the electrodes. Under these circumstances, a characteristic anti-resonance valley is often found in the transmission function.

Dimetallene: a main group or transition metal analog of an alkene.

Dimetallyne: a main group or transition metal analog of an alkyne.

Main group element: an element from the *s*- and *p*-blocks of the periodic table (E). Though carbon is a main group element, our focus here lies on elements outside of carbon, given the pervasiveness of organic backbones in the molecular electronics literature.

Molecular junction: a molecule that bridges at least two metallic electrodes in an electrode-molecule-electrode formation. The molecule can interact with the electrode through covalent, dative, or van der Waals interactions. Single-molecule junctions are composed of a single molecule sandwiched between electrodes, whereas large-area junctions interrogate many molecules organized in a self-assembled monolayer (i.e., one-molecule thick layer) on an electrode surface.

Oligometallane: a main group or transition metal analog of an alkane.

Quantum transport: charge transport dictated by the probability of electronic transmission between electrodes.

Scanning tunneling microscopy break-junction (STM-BJ): a modified scanning tunneling microscopy-based approach for measuring the conductance of single molecules.

Molecular junctions are repeatedly broken and formed in solution thousands of times, allowing for highly reliable and reproducible measurements to be obtained.

clusters of silicon, germanium, and boron define the entire scope of main group backbones that have been studied thus far in quantum transport contexts [26,27,29,30,32]. Despite their structural similarity, heavy tetrel analogs of alkanes exhibit much stronger σ -interactions between their adjacent and vicinal E–E (E = Si, Ge, Sn) bonds due to the increased electropositivity, energy, size, and polarizability of their atomic orbitals [33]. These effects lead to much stronger delocalization in the molecular orbitals relevant to charge transmission, as shown in the highest occupied molecular orbital (HOMO) surfaces in Figure 2A. These orbital interactions have been well-studied in optical absorbance contexts, where increasing oligomer size leads to a red-shifting effect, whereas Si–Si–Si–Si dihedral (ω) rotation toward *syn*-like (ω approaching 0°) conformations lead to blue-shifted absorbance [34].

In the context of quantum transport, the σ -bonds in straight-chain configurations of polysilanes and polygermanes are electronically communicative in ways that resemble π -conjugated organics (Figure 2B) [23–25]. The length-dependent conductance decay (β) value of an oligomeric material is often used to compare the charge transport abilities across material classes of molecular backbones. Repeat units that are resistive to charge transport give high β values, whereas conductive repeat units give shallow β values; alkanes thus carry a steep β value ($\beta = 0.84 \text{ \AA}^{-1}$) [35] compared with π -conjugated alkenes ($\beta = 0.22 \text{ \AA}^{-1}$) [36] and *p*-phenylene rings ($\beta = 0.39\text{--}0.43 \text{ \AA}^{-1}$) [7,37]. Though they are σ -bonded, permethyloligosilanes ($\text{SiMe}_2)_n$ and permethyloligogermanes ($\text{GeMe}_2)_n$ exhibit $\beta = 0.27\text{--}0.39 \text{ \AA}^{-1}$, depending on their end-group substitution [23–25]. Silicon clusters similarly demonstrate appreciable conductance through *transoid/anti*-oriented paths along the cluster backbone [38]. Recently, we have shown that replacing Si atoms with Ge atoms along these paths in sila-adamantane clusters increases conductance [39].

Implications of σ -bond stereoelectronics in quantum transport

The strong σ -interactions across *transoid* ($\omega \sim 165^\circ$) polysilane and polygermane backbones enabled the first observation of stereochemical conductance switching, where mechanical stimuli was used to influence terminal dihedral geometries, and thereby electronic coupling and conductance through the molecular wire [24,25]. While these dihedral configurations always existed in

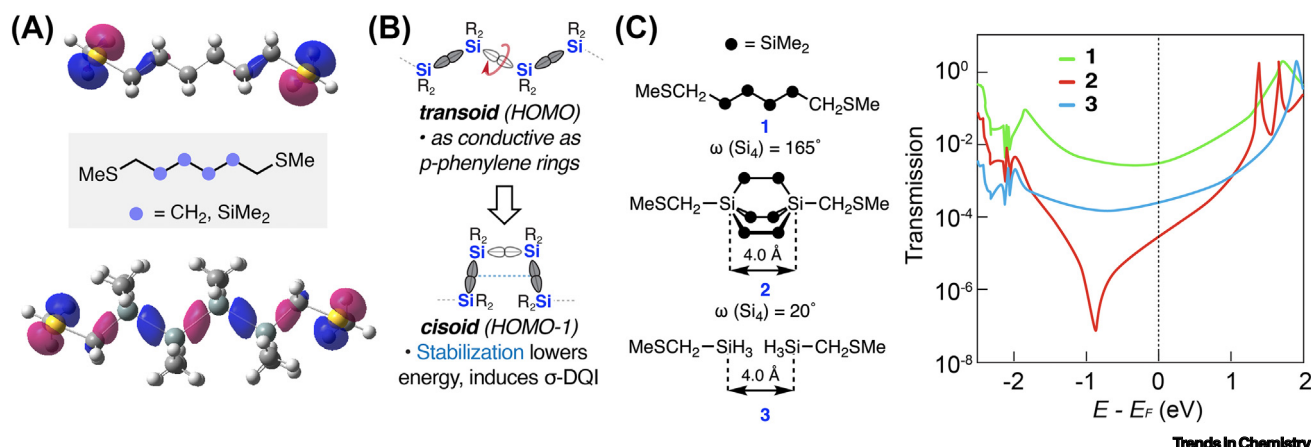


Figure 2. The relationship between oligosilane chain geometry, molecular orbital properties, and electronic transmission. (A) The highest occupied molecular orbital (HOMO) surfaces plotted at the same isovalue for bis(thiomethyl)hexane (top) and bis(methylthiomethyl)-terminated octamethyltetrasilane (bottom). (B) Twisting the oligosilane backbone towards *syn* geometries leads to a HOMO/HOMO-1 inversion due to vicinal hyperconjugative stabilization depicted by the blue dotted line; this geometry change underlies the observed σ -DQI in *cisoid* permethyloligosilanes. (C) Structures studied by Garner *et al.* and their corresponding transmission functions, showing that at E_F (dotted black line), transmission in the *cisoid* cluster **2** is lower than that of 4 Å vacuum gap between the Si centers (**3**). The sharp anti-resonance valley is a hallmark of destructive interference. Data from (C) is reproduced from [28].

alkanes, the poor coupling along the C–C σ -backbone precluded the observation of these stereoelectronic effects. Meanwhile, twisting the polysilane main chain into *cisoid* ($\omega \sim 15\text{--}20^\circ$) configurations in constrained bicyclo[2.2.2]octasilane clusters led to the first report of DQI in σ -bonded systems (Figure 2B,C) [28]. DQI is a uniquely quantum phenomenon that has no bulk electronics analog. As DQI dramatically impacts the magnitude and slope of the transmission function, it can be harnessed for dielectrics and insulators [40], optoelectronics [41] thermoelectrics [42], switches [43,44], and quantum computing [45]. These potential applications motivate the field's interest in studying and understanding DQI.

At short length scales, σ -DQI is more effective at suppressing transmission than π -DQI in the prototypical *meta*-linked benzene, as transmission in the sp^2 σ -channel cannot be turned off. Prior to these studies, it was assumed that DQI occurred only in π -conjugated systems. The origins of σ -DQI in these bicyclic silicon clusters tie back to σ -bond stereoelectronics. As polysilane dihedrals twist from *transoid* to *cisoid*, the erstwhile HOMO experiences stronger energy stabilization and orbital delocalization due to the constructive orbital overlap between vicinal Si–Si σ -bonds (Figure 2B). This stabilization weakens constructive interference with the lowest unoccupied molecular orbital (LUMO), while accentuating destructive interference between the erstwhile HOMO-1 and LUMO at the Fermi energy. σ -DQI in *cisoid* configurations suppresses electronic transmission to the point where their molecular junctions are even more insulating than a vacuum gap at the same electrode separation (Figure 2C). Moreover, the steep slope of the transmission function near E_F gave rise to record-high thermopower values ($\sim 1 \text{ mV K}^{-1}$) [28]. Despite its intrigue, there have been only a few experimental studies on σ -DQI. The groups of Venkataraman and Hong have investigated σ -DQI in alkanes [46,47]. After a thorough computational study on backbone and peripheral substitution of bicyclo[2.2.2]octatetraene (C, Si, Ge) structures, Garner and Solomon concluded that σ -DQI in bicyclic alkane systems can disappear based on linker–electrode contact and substitution compared with heavier tetrel analogs [48,49]. Their prescription indicates the merits in further study of σ -DQI in heavy main group backbones.

Future areas of inquiry for σ -DQI

The champion compounds from Solomon's computational studies are worth targeting to explore whether their predictions hold experimentally. It will also be interesting to explore other precedented bicyclo[2.2.2] motifs with homoatomic Sn [50] or heteroatomic PN [51] backbone compositions in single-molecule junctions. These studies will allow us to consider how valency, spin-orbit coupling, and electronegativity differences may impact destructive σ -quantum interference. σ -DQI is also unexplored in large-area junctions: probing self-assembled monolayers of monofunctionalized bicyclo[2.2.2]octasilane clusters may lead to ultrathin, high-performance dielectrics that operate in the sub-nanometer regime. Finally, it is of interest to design strategies to dynamically control σ -DQI by the reversible control of main chain conformation via external stimuli.

Main group backbones beyond homotetrels

Beyond oligosilane and oligogermanes, alternating silicon–heteroatom (Si–X, X = C, O) backbones have been studied, each offering a different path to achieve molecular insulators with ultrahigh β values beyond that of alkanes. Poly(dimethylsiloxane)s with $\text{SiMe}_2\text{--O}$ repeat units (Figure 3A) give steep β values on both a per-atom ($\beta_{\text{SiO}} = 1.54 \text{ } n^{-1}$) and experimental junction length ($\beta_{\text{SiO}} = 1.45 \text{ } \text{\AA}^{-1}$) basis. This occurs from the stark electronegativity difference between silicon and oxygen that pins orbital density to individual Si–O bonds and diminishes coupling across the backbone [26]. Our recent investigations on poly(dimethylsilmethylene) backbones with $\text{SiMe}_2\text{--CH}_2$ repeat units have shown that, in the absence of strong steric influences, intramolecular London dispersion interactions play a decisive role in influencing junction geometry (Figure 3B) [27]. These concerted interactions stabilize the coiled molecular backbone that

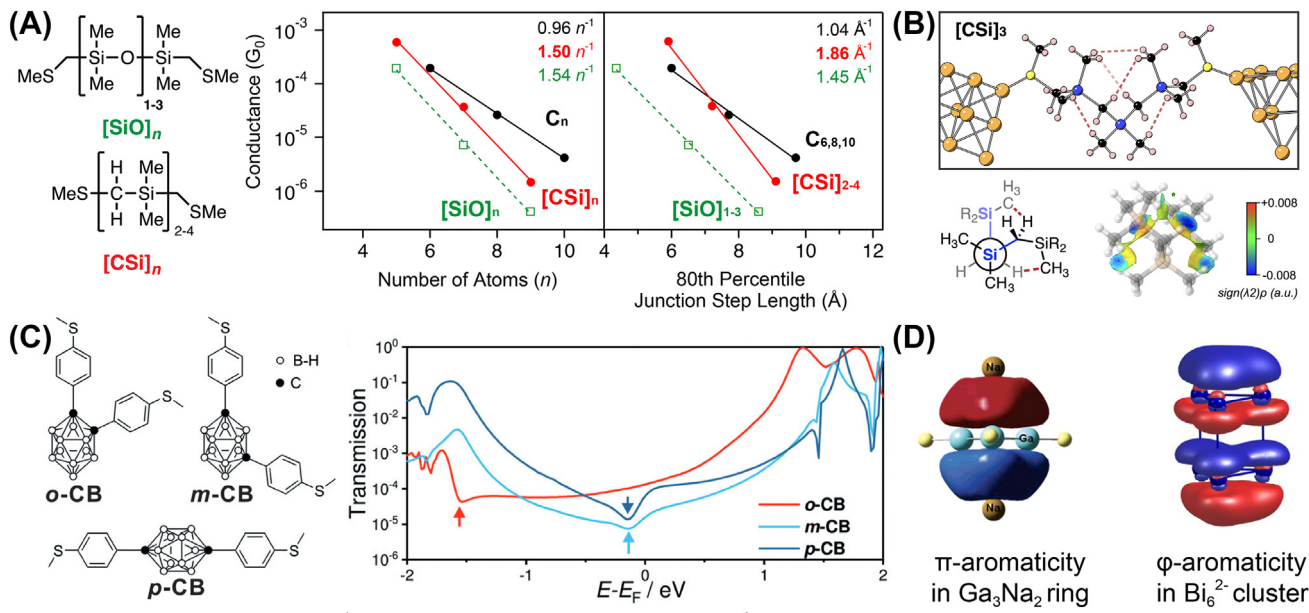


Figure 3. Saturated silicon heteroatom chains, carborane cluster wires, and examples of main group aromaticity. (A) Molecular structures and length-dependent conductance trends of oligo(dimethylsiloxane)s and oligo(dimethylsilmethylene)s. (B) Intramolecular London dispersion interactions (red dotted lines) in a linear carbosilane junction. Newman projections and NCI plot show inter-relation of London dispersion interactions that staple the junction into coiled geometries. (C) Molecular structures of *ortho*-, *meta*-, *para*-linked carboranes with corresponding transmission function curves. Arrows denote anti-resonance valleys indicative of DQI. (D) Simplified computational models of Robinson's π -aromatic Ga_3^{2+} ring and Dehnen's φ -aromatic Bi_6^{2+} cluster. Images reproduced or adapted from [27,32,55,56].

remains intact even as the junction is stretched apart. In this particular case, these coiled backbones are highly insulating and give the highest β values ($\beta = 1.86 \text{ \AA}^{-1}$) that have been observed on an experimental junction length basis (Figure 3A) [27]. Indeed, organosilanes are known from the synthetic literature to carry highly stabilizing dispersion interactions [52]. As we allude to later in this article, it should be possible to use intramolecular London dispersion interactions to design reversible switches or highly conductive systems. We note there are many more polymeric backbones composed of group 13–15 elements that can be functionalized and measured [53,54].

Aside from tetrels, icosahedral B_{10}C_2 carboranes are the only other atomically precise main group cluster class that has been measured (Figure 3C) [32,57,58]. In studies by Hong, Xia, and co-workers, the carboranes were substituted with thioanisole end-groups at the *ortho*-, *meta*-, and *para*-positions and measured via STM-BJ with conductance following the order *ortho* > *para* > *meta* [32]. Interestingly, DQI anti-resonances were found between the HOMO and LUMO levels, regardless of where the thioanisole linkers were installed (Figure 3C). The chemical basis for this observation is unclear; is it a consequence of the icosahedral symmetry, three center-two electron bonding configuration, three-dimensional aromaticity, or another facet of carboranes? Broader inquiry into related polyhedral boron clusters will deepen our understanding of this phenomenon [59]. Finally, in organic backbones, it has been determined that strong aromatic character diminishes molecular conductance relative to quinoidal forms [60], whereas anti-aromaticity raises conductance [61]. The concepts of σ -, π -, and φ -metalloaromaticity are gaining traction in cyclic main group molecules and clusters (Figure 3D) [55,56,62–64]; it will be of great interest to consider whether and how these flavors of main group aromaticity may influence quantum transport.

Multiply bonded main group backbones

The previous section described how saturated main group backbones can be as conductive as π -conjugated *p*-phenylene rings. Can we make main group backbones that are more conductive than their π -conjugated organic analogs? In our view, unsaturated or multiply bonded main group backbones (Figures 1C and 4) are the most promising candidates to meet this objective, though they are unexplored in molecular electronic contexts. Since the first isolation of a disilene by West, Fink, and Michl [65] and diphosphene by Yoshifuji and coworkers [66], main group chemists have diligently expanded the scope of homo- and heteroatomic group 13, 14, 15, and 16 analogs of alkenes and alkynes [67–69]. Similar to how low-valent main group compounds have contributed significantly to the burgeoning field of main group catalysis [70], we believe that taking advantage of the unique structure and bonding in unsaturated main group species will similarly impact molecular electronics (Figure 4).

Despite their resemblance, multiply bonded main group species are distinct from their organic congeners in terms of their structure and bonding (Figure 5A). Carbon's position in the second row of the periodic table lies at the heart of these differences. As Dreiss and Grützmacher stated, despite its familiarity, carbon should be conceived as the 'exotic' tetrel out of the group 14 elements due to its strong bonding overlap and triplet carbene ground state [67]. By virtue of having a filled 2p core, the rest of the tetrads experience poor bonding overlap and singlet tetrelene ground states, with bond strengths that weaken down the periodic table [71]. These differences in tetrelene ground state manifest in their non-classical bonding geometries (Figure 5B): while C=C bonds are planar, E=E bonds adopt conformationally flexible *trans*-bent and twisted geometries. These conformations have been rationalized by Carter, Goddard, Malrieu, and Trinquier [72,73] and distorted Jahn-Teller [68,74] models.

The promise of main group π -bonds in molecular electronics

As a consequence of their weak bonding overlap, multiply-bonded main group species tend to exhibit smaller HOMO–LUMO gaps descending the periodic table (Figure 5B). Optical gaps of **dimetallenes** and related species have been reported in the visible and near-infrared regimes, significantly red-shifted from their organic counterparts [75–77]. These small HOMO–LUMO

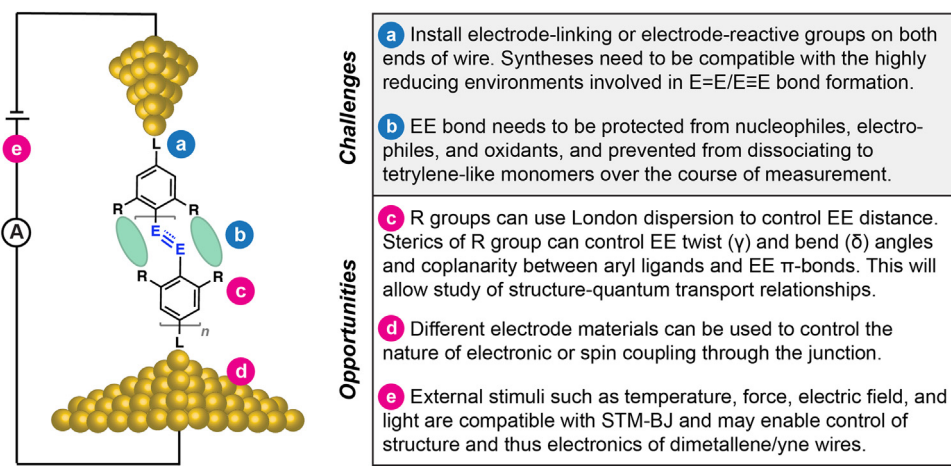


Figure 4. Challenges and opportunities to studying dimetallene and dimetallyne-based wires via the scanning tunneling microscopy break-junction (STM-BJ) technique, broken down from an anatomical perspective of the molecular junction.

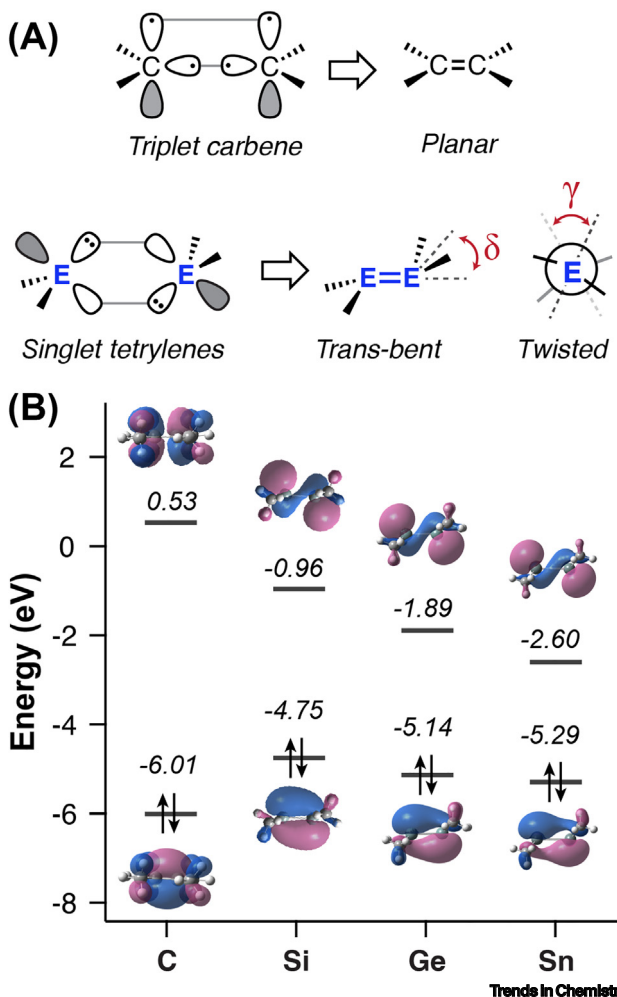


Figure 5. Differences in the π -bonding nature of ethylene versus dimetallenes. (A) Dimetallenes and dimetallynes may adopt planar to *trans*-bent (δ) conformations that can also twist (γ). Especially going down the periodic table, other isomeric structures may also be adopted. (B) Highest occupied molecular orbital and lowest unoccupied molecular orbital levels of $\text{Me}_2\text{E}=\text{EMe}_2$ ($\text{E} = \text{C}, \text{Si}, \text{Ge}, \text{Sn}$) calculated at the B3LYP-D3(BJ)/def2tzvp level of theory, with all surfaces plotted at isovalue = 0.03. The alkene is planar, while the dimetallenes become increasingly *trans*-bent down the periodic table.

gaps may lead to charge transport that is orders of magnitude more transmissive than their carbon-based analogs [9]. If the HOMO energies are high enough or LUMO energies are low enough, these wires may engage in resonant transport if the molecular orbital resonance energetically aligns with the electrode's Fermi energy. Resonant transport is exciting because it can be harnessed for molecular wires where electron flow occurs over long length scales with minimal loss in conductance [78,79]. Resonant transport is also a key component in the design of molecular thermoelectrics with high zT values due to their high Seebeck coefficient and conductivity [80,81] and voltage-activated molecular switches with large on/off ratios [44].

Despite their promise, the use of multiply bonded main group species as electronic materials has been largely unexplored. In our view, this is for several reasons. First, relative to organic compounds, the synthesis and isolation of dimetallenes and **dimetallynes** is not trivial. Advanced π -conjugated organic building blocks can be procured from petrol feedstocks; obtaining similarly complex main group compounds requires more synthetic effort. Moreover, these compounds can be highly air-sensitive and more difficult to isolate and study. Second, while bulky organic ligands kinetically stabilize the $\text{E}=\text{E}$ bond, they also hinder efficient transport in conventional

thin-film devices (Figure 6A). These ligands prevent close contact between E=E bonds necessary for efficient charge transfer, while also acting as charge traps for intermolecular transport [82]. Tamao and coworkers described the only example of using disilenes in the active layers of thin-film devices, but characterized the electroluminescence performance as quite low [83]. In our view, these bulky ligands will always pose a fundamental limit to using dimetallenes or dimetallynes in thin-film devices. Fortunately, these points should be a non-issue in single-molecule electronics. This is where the opportunity lies.

Challenges, potential solutions, and opportunities in realizing multiply-bonded main group molecular electronics

In single-molecule electronics, the relevant factor is electronic coupling through the molecule, rather than electronic coupling between molecules. Figure 6B shows a schematic depiction of such a single-molecule junction based on Tamao's (HexO)MEind-stabilized phenylene-disilene oligomers. Provided that electrode-binding or electrode-reactive end-groups (Figure 1A) can be installed at accessible locations in the backbone termini [9,16], the alkyl sheath should not interfere with electrode–molecule contact. Cea, Serrano, Nichols, and coworkers have found similarly sheathed supramolecular systems readily make contact with electrodes [84]. Though some dimetallenes and dimetallynes are reported to be air-stable for short periods, measurements under rigorously air-free conditions will provide confidence that the molecule remains intact under measurement conditions. One solution arises from recent work by Inkpen and coworkers, who described a glovebox STM-BJ measurement system that will not only address these measurement requirements, but also permit air-sensitive metal electrodes beyond gold to be used [85]. There are several ligand design considerations (Figure 4) to keep in mind that will be specific to measuring reactive dimetallenes and dimetallynes in molecular junctions.

First, within these aryl ligands, we will need to install electrode-binding or electrode-reactive end-groups at positions that are electronically communicative (i.e., the *para* position) through the E=E bond (Figure 4A) [9]. The highly reducing synthetic environments often used to make E=E and E≡E bonds have limited functional group tolerance, so the installation of these linker groups will need to be carefully designed.

Second, we should initiate these investigations from ligands that facilitate strong electronic coupling between the E=E bond and the electrodes. Aryl ligands with bulky *ortho* substituents (Figure 4B)

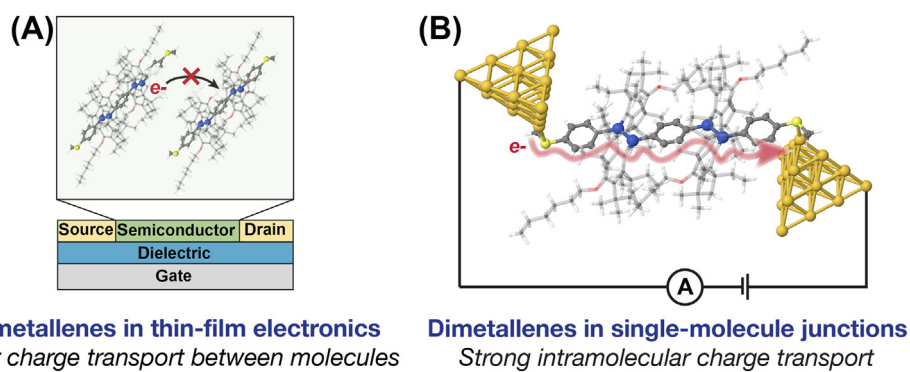


Figure 6. Advantages of investigating dimetallene charge transport in single-molecule junctions compared to thin-film devices. (A) Schematic for a thin-film transistor with a model phenylene-disilene oligomer. The bulky ligand shell needed to stabilize the disilene prevents the disilene moieties from getting close enough to promote effective intermolecular charge transport. (B) Schematic for the same model phenylene-disilene oligomer in a single-molecule junction, where effective charge transport through the molecular backbone should not be impacted by the ligand shroud.

are frequently deployed to stabilize the dimetallene/yne and may at least partially align the metal-linker bond with the E=E/E≡E backbone [68,69,77]. There may also be opportunities to modify the structure of bulky N-heterocyclic carbenes so they have an electrode-binding moiety [86].

Third, the E=E/E≡E bond should be kinetically protected, not only from reaction from O₂, but also from the electrodes. Due to their amphiphilic nature, these highly reactive bonds may either make direct contact or react with Au electrodes under applied voltage bias [87]. The alkyl sheath will be critical for keeping the E=E/E≡E bonds intact as current passes through.

Finally, we should be careful to select dimetallene/yne structures that maintain their multiply bonded nature in solution. Their dimeric form is required for measurement across the wire, so care should be taken in considering the E=E bond strength, singlet-triplet energy gap of the carbene, and the sterics and dispersion of the ligand group [88–90]. Many dimetallenes/ynes are multiply bonded in the solid state, yet exist in equilibrium with their tetrylene-like form in solution. If this is the case, this solution equilibrium will be driven to the carbene state if the carbene binds to the electrode surface. Conversely, this can be viewed as a feature rather than a bug if the intent is to study heavy carbene analogs as electrode anchors for molecular electronics [86,91]. Careful ligand design should also account for the low barriers to E-Z and dyotropic isomerization in dimetallenes [87,92]. Of course, these are just starting points; our notions of molecular design will evolve as the field begins investigating suitable dimetallene and dimetallyne candidates for STM-BJ interrogation.

The unique structure and bonding considerations of unsaturated main group compounds will likely create new opportunities in single-molecule electronics (Figure 4C–E). The 2,4,6-triisopropylphenyl (Trip) and similar ligands have led to the isolation of solution-stable Si=Si, Ge=Ge, and Sn=Sn species [69,93]. Systematic study down a *p*-block group using the same ligand structure will allow us to evaluate how quantum transport is impacted by the weakening bond strength (and smaller HOMO-LUMO gap), increasing inert-pair effect, and increasing spin-orbit coupling as the dimetallene identity descends the periodic table. These explorations may expand to studying heavy RE≡ER ditetryne series [94–97], formally neutral disilicon species [98], heterotetrel E=E' (E,E'=Si, Ge, Sn) bonds, allene analogs [99], and the radical cations and anions that will result from their oxidation or reduction [69]. It will also be worth exploring multiply bonded group 13 and 15 species as B=B, Al=Al, Ga=Ga, P=P, As=As, Sb=Sb, and related heterodimetallenes [69].

The balance between steric bulk and dispersion interactions carried by the ligand exerts a considerable influence over dimetallene and dimetallyne geometry (Figure 4C). We can thus vary the ligand structure to tune E=E/E≡E bond length, bend angle (i.e., from planar to *trans*-bent), twist angle (Figure 5), bond order, and diradical character [100], all of which are likely to influence quantum transport. Moreover, the conformationally flexible nature of main group analogs of alkenes and alkynes suggest we may be able to dynamically control these structural parameters with temperature, mechanical stimuli, light, or electric field strength (Figure 4E). For example, disilenes have demonstrated reversible thermochromism and temperature-induced transitions to triplet diradical states [101–103]. Such systems may lead to stimuli-responsive molecular junction switches with large differences in electronic coupling [104]. Finally, it will be worth investigating oligomeric forms of dimetallenes and interrogating their length-dependent conductance decay. Weidenbruch and coworkers reported disilene analogs of polyacetylene [105], whereas the groups of Scheschkewitz and Tamao have reported disilene analogs [76,77,106,107] of organic oligo(phenylene vinylene) wires. The high HOMO energies that will likely accompany these disilene wires may give resonant transport independent of wire length, leading to molecular wires with

zero or negative β values [78, 108]. Moreover, if the twist angle of such oligomeric structures can be regulated by ligand design or external stimuli, these materials may demonstrate desirable chiral-induced spin selectivity effects in molecular junctions, particularly if spin-polarized electrodes are applied (Figure 4D) [109].

Concluding remarks

Main group compounds exhibit unique orbital interactions, bonding geometries, and stereoelectronics distinct from organic systems. Exploring quantum transport in main group backbones has thus unveiled novel phenomena and sparked new concepts in molecular electronics. In our view, these findings represent only the tip of the iceberg. Intriguing questions have emerged from these studies that are propelling us into uncharted territory (see **Outstanding questions**). Expanding into this territory will require us to deepen the chemical space for main group elements studied in molecular junctions. Investigating new backbone chains and clusters spanning the *p*-block elements will be essential, alongside exploring the quantum transport properties of main group analogs of alkenes and alkynes. Collaboration between main group chemists and single-molecule electronics practitioners will drive advancements in this untapped area for discovery in molecular electronics.

Acknowledgments

The work and concepts described here have been supported by the National Science Foundation (CHE-2340979), the Air Force Office of Scientific Research (FA9550-22-1-0404), and the Cottrell Scholars Program (CS-CSA-2024-069). M.O.H. is supported by the donors of the American Chemical Society Petroleum Research Fund (65042-DNI7).

Declaration of interests

The authors declare no competing interests.

References

- Aviram, A. and Ratner, M.A. (1974) Molecular rectifiers. *Chem. Phys. Lett.* 29, 277–283
- Reed, M.A. *et al.* (1997) Conductance of a molecular junction. *Science* 278, 252–254
- Wold, D.J. and Frisbie, C.D. (2000) Formation of metal–molecule–metal tunnel junctions: microcontacts to alkanethiol monolayers with a conducting AFM tip. *J. Am. Chem. Soc.* 122, 2970–2971
- Cui, X.D. *et al.* (2001) Reproducible measurement of single-molecule conductivity. *Science* 294, 571–574
- Smit, R.H.M. *et al.* (2002) Measurement of the conductance of a hydrogen molecule. *Nature* 419, 906–909
- Xu, B. and Tao, N.J. (2003) Measurement of single-molecule resistance by repeated formation of molecular junctions. *Science* 301, 1221–1223
- Venkataraman, L. *et al.* (2006) Dependence of single-molecule junction conductance on molecular conformation. *Nature* 442, 904–907
- Chiechi, R.C. *et al.* (2008) Eutectic gallium–indium (EGaIn): a moldable liquid metal for electrical characterization of self-assembled monolayers. *Angew. Chem. Int. Ed.* 47, 142–144
- Su, T.A. *et al.* (2016) Chemical principles of single-molecule electronics. *Nat. Rev. Mater.* 1, 16002
- Gehring, P. *et al.* (2019) Single-molecule quantum-transport phenomena in break junctions. *Nat. Rev. Phys.* 1, 381–396
- Evers, F. *et al.* (2020) Advances and challenges in single-molecule electron transport. *Rev. Mod. Phys.* 92, 35001
- Sun, L. *et al.* (2014) Single-molecule electronics: from chemical design to functional devices. *Chem. Soc. Rev.* 43, 7378–7411
- Cheng, Z.-L. *et al.* (2011) In situ formation of highly conducting covalent Au–C contacts for single-molecule junctions. *Nat. Nanotechnol.* 6, 353–357
- Hong, W. *et al.* (2012) Trimethylsilyl-terminated oligo(phenylene ethynylene)s: an approach to single-molecule junctions with covalent Au–C σ -bonds. *J. Am. Chem. Soc.* 134, 19425–19431
- Hines, T. *et al.* (2013) Controlling formation of single-molecule junctions by electrochemical reduction of diazonium terminal groups. *J. Am. Chem. Soc.* 135, 3319–3322
- Starr, R.L. *et al.* (2020) Gold–carbon contacts from oxidative addition of aryl iodides. *J. Am. Chem. Soc.* 142, 7128–7133
- Li, Y. *et al.* (2022) In situ monitoring of transmetallation in electric potential-promoted oxidative coupling in a single-molecule junction. *CCS Chem.* 5, 191–199
- Ismail, A.K. *et al.* (2017) Side-group-mediated mechanical conductance switching in molecular junctions. *Angew. Chem. Int. Ed.* 56, 15378–15382
- Daaoub, A. *et al.* (2023) Not so innocent after all: interfacial chemistry determines charge-transport efficiency in single-molecule junctions. *Angew. Chem.* 135, e202302150
- Zhao, Z.-H. *et al.* (2020) Single-molecule conductance through an isolectronic B–N substituted phenanthrene junction. *J. Am. Chem. Soc.* 142, 8068–8073
- Baghernejad, M. *et al.* (2019) Quantum interference enhanced chemical responsivity in single-molecule dithienoboropin junctions. *Chem. Eur. J.* 25, 15141–15146
- Skipper, H.E. *et al.* (2021) Hard–soft chemistry design principles for predictive assembly of single-molecule–metal junctions. *J. Am. Chem. Soc.* 143, 16439–16447
- Klausen, R.S. *et al.* (2012) Conductive molecular silicon. *J. Am. Chem. Soc.* 134, 4541–4544
- Su, T.A. *et al.* (2015) Stereoelectronic switching in single-molecule junctions. *Nat. Chem.* 7, 215–220
- Su, T.A. *et al.* (2015) Single-molecule conductance in atomically precise germanium wires. *J. Am. Chem. Soc.* 137, 12400–12405
- Li, H. *et al.* (2017) Extreme conductance suppression in molecular siloxanes. *J. Am. Chem. Soc.* 139, 10212–10215
- Hight, M.O. *et al.* (2024) Intramolecular London dispersion interactions in single-molecule junctions. *J. Am. Chem. Soc.* 146, 4716–4726

Outstanding questions

Broadening the scope of main group molecular wires: what new insights will be revealed by studying polymers with other *p*-block elements in the main chain? How might σ -, π -, or ϕ -aromaticity manifest in quantum transport contexts? Can we use intramolecular London dispersion interactions to install new functions into molecular junctions?

Destructive quantum interference in main group species: can we develop a straightforward understanding for when σ -DQI will give a strong anti-resonance valley near E_F like we can predict for π -DQI in organic systems? Does σ -DQI occur in elements beyond silicon, in heavier tetrals, triels, or pnictogens, and if so, what will define their similarities and differences? Can we make σ -DQI a dynamic property of molecular junctions that can be attenuated or strengthened in response to external stimuli?

Unsaturated main group electronics: what new transport phenomena will emerge from studying dimetallene and dimetallyne wires composed of varying *p*-block elements? Can we modify generic ligand classes that will kinetically stabilize a broad range of dimetalenes and dimetallynes and enable their connection to electrodes? How will diradical character, bond length, twist angle, and bend angle about the E=E/E \equiv E bond impact quantum transport? Can we use external stimuli to influence junction structure and bonding?

28. Garner, M.H. *et al.* (2018) Comprehensive suppression of single-molecule conductance using destructive σ -interference. *Nature* 558, 416–419

29. Su, T.A. *et al.* (2017) Silane and germane molecular electronics. *Acc. Chem. Res.* 50, 1088–1095

30. Siu, T.C. *et al.* (2021) Single-cluster electronics. *Phys. Chem. Chem. Phys.* 23, 9643–9659

31. Datta, S. *Quantum Transport: Atom to Transistor*, Cambridge University Press

32. Tang, C. *et al.* (2019) Multicenter-bond-based quantum interference in charge transport through single-molecule carborane junctions. *Angew. Chem. Int. Ed.* 58, 10601–10605

33. Schepers, T. and Michl, J. (2002) Optimized ladder C and ladder H models for sigma conjugation: chain segmentation in polysilanes. *J. Phys. Org. Chem.* 15, 490–498

34. Tsuji, H. *et al.* (2003) Recent experimental and theoretical aspects of the conformational dependence of UV absorption of short chain peralkylated oligosilanes. *J. Organomet. Chem.* 685, 9–14

35. Li, X. *et al.* (2006) Conductance of single alkanedithiols: conduction mechanism and effect of molecule–electrode contacts. *J. Am. Chem. Soc.* 128, 2135–2141

36. He, J. *et al.* (2005) Electronic decay constant of carotenoid polyenes from single-molecule measurements. *J. Am. Chem. Soc.* 127, 1384–1385

37. Li, S. *et al.* (2021) Transition between nonresonant and resonant charge transport in molecular junctions. *Nano Lett.* 21, 8340–8347

38. Li, H. *et al.* (2018) Large variations in the single-molecule conductance of cyclic and bicyclic silanes. *J. Am. Chem. Soc.* 140, 15080–15088

39. Cardenas, Imex Aguirre *et al.* (2023) Installing quaternary germanium centers in sila-diamondoid cores via skeletal isomerization. *J. Am. Chem. Soc.* 145, 20588–20594

40. Bergfield, J.P. *et al.* (2015) Harnessing quantum interference in molecular dielectric materials. *ACS Nano* 9, 6412–6418

41. Parenti, K. *et al.* (2022) The role of quantum interference in intramolecular singlet fission. *ChemRxiv*, Published online June 8, 2022. <https://doi.org/10.26434/chemrxiv-2022-20q55>

42. Li, X. *et al.* (2019) Experimental investigation of quantum interference in charge transport through molecular architectures. *J. Mater. Chem. C* 7, 12790–12808

43. Baer, R. and Neuhauser, D. (2002) Phase coherent electronics: a molecular switch based on quantum interference. *J. Am. Chem. Soc.* 124, 4200–4201

44. Greenwald, J.E. *et al.* (2021) Highly nonlinear transport across single-molecule junctions via destructive quantum interference. *Nat. Nanotechnol.* 16, 313–317

45. Jensen, P.W.K. *et al.* (2022) Toward quantum computing with molecular electronics. *J. Chem. Theory Comput.* 18, 3318–3326

46. Zhang, B. *et al.* (2021) Destructive quantum interference in heterocyclic alkanes: the search for ultra-short molecular insulators. *Chem. Sci.* 12, 10299–10305

47. Ye, J. *et al.* (2022) Highly insulating alkane rings with destructive σ -interference. *Sci. China Chem.* 65, 1822–1828

48. Garner, M.H. *et al.* (2022) Substituent control of σ -interference effects in the transmission of saturated molecules. *ACS Phys. Chem. Au* 2, 282–288

49. Garner, M.H. *et al.* (2018) The bicyclo[2.2.2]octane motif: a class of saturated group 14 quantum interference based single-molecule insulators. *J. Phys. Chem. Lett.* 9, 6941–6947

50. Steller, B.G. *et al.* (2020) Reductive dehydrocoupling of diphenyltin dihydride with LiAlH₄: selective synthesis and structures of the first bicyclo[2.2.1]heptastannane-1,4-diide and bicyclo[2.2.2]octastannane-1,4-diide. *Chem. Commun.* 56, 336–339

51. Bedard, J. *et al.* (2023) A robust, divalent, phosphaza-bicyclo[2.2.2]octane connector provides access to cage-dense inorganic polymers and networks. *J. Am. Chem. Soc.* 145, 7569–7579

52. Pollici, R. and Chen, P. (2019) A universal quantitative descriptor of the dispersion interaction potential. *Angew. Chem. Int. Ed.* 58, 9758–9769

53. Priegert, A.M. *et al.* (2016) Polymers and the P-block elements. *Chem. Soc. Rev.* 45, 922–953

54. Vidal, F. and Jäkle, F. (2019) Functional polymeric materials based on main-group elements. *Angew. Chem. Int. Ed.* 58, 5846–5870

55. Wang, Y. and Robinson, G.H. (2007) Organometallics of the group 13 M–M bond (M = Al, Ga, In) and the concept of metalloaromaticity. *Organometallics* 26, 2–11

56. Peerless, B. *et al.* (2023) φ -Aromaticity in prismatic [Bi₆]-based clusters. *Nat. Chem.* 15, 347–356

57. Lin, L. *et al.* (2021) Spectral clustering to analyze the hidden events in single-molecule break junctions. *J. Phys. Chem. C* 125, 3623–3630

58. Xu, S.-N. *et al.* (2023) Conductance of σ -carborane-based wires with different substitution patterns. *Dalton Trans.* 52, 4349–4354

59. King, R.B. (2001) Three-dimensional aromaticity in polyhedral boranes and related molecules. *Chem. Rev.* 101, 1119–1152

60. Chen, W. *et al.* (2014) Aromaticity decreases single-molecule junction conductance. *J. Am. Chem. Soc.* 136, 918–920

61. Breslow, R. and Foss Jr., F.W. (2008) Charge transport in nanoscale aromatic and antiaromatic systems. *J. Phys. Condens. Matter* 20, 374104

62. Popov, I.A. *et al.* (2018) Usefulness of the σ -aromaticity and σ -antiaromaticity concepts for clusters and solid-state compounds. *Chem. Eur. J.* 24, 292–305

63. Li, X.-W. *et al.* (1995) Metallic system with aromatic character. Synthesis and molecular structure of Na₂[{2,4,6-Me₃C₆H₂}(2C₆H₃]Ga]3 the first cyclogallane. *J. Am. Chem. Soc.* 117, 7578–7579

64. Abersfelder, K. *et al.* (2010) A tricyclic aromatic isomer of hexasilabenzene. *Science* 327, 564–566

65. West, R. *et al.* (1981) Tetramesityldisilene, a stable compound containing a silicon–silicon double bond. *Science* 214, 1343–1344

66. Yoshifuiji, M. *et al.* (1981) Synthesis and structure of bis[2,4,6-tri-*t*-butylphenyl]diphosphene: isolation of a true phosphobenzene. *J. Am. Chem. Soc.* 103, 4587–4589

67. Driess, M. and Grützmacher, H. (1996) Main group element analogues of carbenes, olefins, and small rings. *Angew. Chem. Int. Ed. Eng.* 35, 828–856

68. Power, P.P. (1999) π -Bonding and the lone pair effect in multiple bonds between heavier main group elements. *Chem. Rev.* 99, 3463–3504

69. Fischer, R.C. and Power, P.P. (2010) π -Bonding and the lone pair effect in multiple bonds involving heavier main group elements: developments in the new millennium. *Chem. Rev.* 110, 3877–3923

70. Inoue, S. *et al.* (2022) Main group catalysis. *Eur. J. Inorg. Chem.* 2022, e202200414

71. Goddard, W.A. and Harding, L.B. (1978) The description of chemical bonding from ab initio calculations. *Annu. Rev. Phys. Chem.* 29, 363–396

72. Carter, E.A. and Goddard, W.A.I. (1986) Relation between singlet-triplet gaps and bond energies. *J. Phys. Chem.* 90, 998–1001

73. Trinquier, G. and Malrieu, J.P. (1987) Nonclassical distortions at multiple bonds. *J. Am. Chem. Soc.* 109, 5303–5315

74. Kira, M. (2011) Distortion modes of heavy ethylenes and their anions: π – Σ^* orbital mixing model. *Organometallics* 30, 4459–4465

75. Kobayashi, M. *et al.* (2010) Air-stable, room-temperature emissive disilenes with π -extended aromatic groups. *J. Am. Chem. Soc.* 132, 15162–15163

76. Obeid, N.M. *et al.* (2017) (Oligo)aromatic species with one or two conjugated Si–Si bonds: near-IR emission of anthracenyl-bridged tetrasiladiene. *Dalton Trans.* 46, 8839–8848

77. Li, L. *et al.* (2015) Coplanar oligo(p-phenylenedisilyleylene)s as Si=Si analogues of oligo(p-phenylenevinylene)s: evidence for extended π -conjugation through the carbon and silicon π -frameworks. *J. Am. Chem. Soc.* 137, 15026–15035

78. Zang, Y. *et al.* (2018) Resonant transport in single diketopyrrolopyrrole junctions. *J. Am. Chem. Soc.* 140, 13167–13170

79. Lörtscher, E. and Riel, H. (2010) Molecular electronics – resonant transport through single molecules. *Chim. Int. J. Chem.* 64, 376–382

80. Sangtarash, S. and Sadeghi, H. (2020) Radical enhancement of molecular thermoelectric efficiency. *Nanoscale Adv.* 2, 1031–1035

81. Kim, Y. *et al.* (2014) Electrostatic control of thermoelectricity in molecular junctions. *Nat. Nanotechnol.* 9, 881–885

82. Haneef, H.F. *et al.* (2020) Charge carrier traps in organic semiconductors: a review on the underlying physics and impact on electronic devices. *J. Mater. Chem. C* 8, 759–787

83. Tamao, K. *et al.* (2012) The first observation of electroluminescence from di(2-naphthyl)disilene, an SiSi double bond-containing π -conjugated compound. *Chem. Commun.* 48, 1030–1032

84. Herrer, L. *et al.* (2023) Sheathed molecular junctions for unambiguous determination of charge-transport properties. *Adv. Mater. Interfaces* 10, 2300133

85. Miao, Z. *et al.* (2022) Charge transport across dynamic covalent chemical bridges. *Nano Lett.* 22, 8331–8338

86. Doud, E.A. *et al.* (2018) In situ formation of N-heterocyclic carbene-bound single-molecule junctions. *J. Am. Chem. Soc.* 140, 8944–8949

87. Kira, M. (2012) Bonding and structure of disilenes and related unsaturated group-14 element compounds. *Proc. Jpn. Acad. Ser. B* 88, 167–191

88. Abe, T. *et al.* (2012) New isolable dialkylsilylene and its isolable dimer that equilibrate in solution. *J. Am. Chem. Soc.* 134, 20029–20032

89. Schmedake, T.A. *et al.* (1999) Reversible transformation between a diaminosilylene and a novel disilene. *J. Am. Chem. Soc.* 121, 9479–9480

90. Sakamoto, K. *et al.* (1997) Generation and trapping of bis(dialkylamino)silylenes: experimental evidence for bridged structure of diaminosilylene dimers. *Bull. Chem. Soc. Jpn.* 70, 253–260

91. Cradden, C.M. *et al.* (2014) Ultra stable self-assembled monolayers of N-heterocyclic carbenes on gold. *Nat. Chem.* 6, 409–414

92. Yokelson, H.B. *et al.* (1990) 1,2-Diaryl rearrangement in tetraaryldisilenes. *Organometallics* 9, 1005–1010

93. Stennett, C.R. *et al.* (2021) Designing a solution-stable distannene: the decisive role of London dispersion effects in the structure and properties of $\{Sn(C_6H_2-2,4,6-Cy_3)_2\}_2$ (Cy = cyclohexyl). *J. Am. Chem. Soc.* 143, 21478–21483

94. Stender, M. *et al.* (2002) Synthesis and characterization of a digermanium analogue of an alkyne. *Angew. Chem.* 114, 1863–1865

95. Phillips, A.D. *et al.* (2002) Synthesis and characterization of 2,6-dipp₂-H₃C₆SnC₆H₃-2,6-dipp₂ (dipp = C₆H₃-2,6-Pr₂): a tin analogue of an alkyne. *J. Am. Chem. Soc.* 124, 5930–5931

96. Sekiguchi, A. *et al.* (2004) A stable compound containing a silicon-silicon triple bond. *Science* 305, 1755–1757

97. Sasamori, T. *et al.* (2008) Synthesis and reactions of a stable 1,2-diaryl-1,2-dibromodisilene: a precursor for substituted disilenes and a 1,2-diaryldisilene. *J. Am. Chem. Soc.* 130, 13856–13857

98. Wang, Y. *et al.* (2008) A stable silicon(0) compound with a Si=Si double bond. *Science* 321, 1069–1071

99. Ishida, S. *et al.* (2003) A stable silicon-based allene analogue with a formally Sp-hybridized silicon atom. *Nature* 421, 725–727

100. Liptrot, D.J. and Power, P.P. (2017) London dispersion forces in sterically crowded inorganic and organometallic molecules. *Nat. Rev. Chem.* 1, 0004

101. West, R. (1984) Isolable compounds containing a silicon-silicon double bond. *Science* 225, 1109–1114

102. Kira, M. and Iwamoto, T. (2006) Progress in the chemistry of stable disilenes. *Adv. Organomet. Chem.* 54, 73–148

103. Kostenko, A. *et al.* (2015) Observation of a thermally accessible triplet state resulting from rotation around a main-group π bond. *Angew. Chem. Int. Ed.* 54, 12144–12148

104. Stuyver, T. *et al.* (2018) Diradical character as a guiding principle for the insightful design of molecular nanowires with an increasing conductance with length. *Nano Lett.* 18, 7298–7304

105. Weidenbruch, M. *et al.* (1997) Hexaaryltetrasilabuta-1,3-diene: a molecule with conjugated Si-Si double bonds. *Angew. Chem. Int. Ed. Engl.* 36, 2503–2504

106. Bejan, I. and Scheschkewitz, D. (2007) Two Si-Si double bonds connected by a phenylene bridge. *Angew. Chem. Int. Ed.* 46, 5783–5786

107. Fukazawa, A. *et al.* (2007) Coplanar oligo(p-phenylenedisilylene)s based on the octaethyl-substituted s-hydridacetyl groups. *J. Am. Chem. Soc.* 129, 14164–14165

108. Xu, W. *et al.* (2019) Unusual length dependence of the conductance in cumulene molecular wires. *Angew. Chem. Int. Ed.* 58, 8378–8382

109. Naaman, R. and Waldeck, D.H. (2012) Chiral-induced spin selectivity effect. *J. Phys. Chem. Lett.* 3, 2178–2187